



The Impact of Climate Change on the Reinforcement Durability of Concrete Bridge Structures

Riyadh Alsultani^{1,*}, Qahtan Adnan Saber², Ahmed Ashor Al-Saadi¹, Omran I Mohammed¹, Sabah Mohammed Abed¹, Raghda Ali Naser¹, Alaa Hussein¹, Fatima Muslim¹, Haneen Fadhil¹, Ibtisam R. Karim³ and Saleh I. Khassaf⁴

¹Department of Building and Construction Techniques Engineering, Al-Mustaqbal University, 51001, Hilla, Iraq

²Civil Department, Kirkuk Technical Institute, Northern Technical University, Kirkuk, Iraq

³Department of Civil Engineering, University of Technology, Baghdad, Iraq

⁴Department of Civil Engineering, University of Basrah, Basrah, 61001, Iraq

Abstract:

Background: Climate change poses significant challenges to the durability of concrete bridge structures, particularly regarding the corrosion of reinforcement. Iraq, due to its geographical location, is particularly vulnerable to greenhouse gas emissions, with carbon dioxide (CO₂) being the most prominent. The country's heavy reliance on energy resources like coal, gas, and oil exacerbates air pollution, further compounding environmental concerns. Corrosion of reinforcement in concrete infrastructure, including bridges, is primarily driven by the presence of atmospheric CO₂. The risk of corrosion increases with rising CO₂ levels associated with global warming, leading to potentially catastrophic damage that is costly to repair.

Methods: This study employs a probabilistic technique to predict the damage potential of concrete infrastructure exposed to carbonation resulting from elevated temperatures and CO₂ concentrations.

Results: The findings reveal a significant increase in the risk of damage from carbonation in certain regions of Iraq, with potential rises exceeding 400% by 2100. Additionally, rising temperatures elevate the likelihood of chloride impact by up to 15% over the same period. However, these assessments do not consider changes in ocean acidity in marine exposure, which could further exacerbate the effects of climate change on concrete infrastructure.

Conclusion: The results underscore the urgent need for proactive measures to mitigate the impact of rising atmospheric CO₂ levels on the durability of bridge structures in the face of climate change.

Keywords: Reinforcement durability, Climate change, Energy production, Greenhouse gases, CO₂ levels, Geothermal.

© 2024 The Author(s). Published by Bentham Open.

This is an open access article distributed under the terms of the Creative Commons Attribution 4.0 International Public License (CC-BY 4.0), a copy of which is available at: <https://creativecommons.org/licenses/by/4.0/legalcode>. This license permits unrestricted use, distribution, and reproduction in any medium, provided the original author and source are credited.

*Address correspondence to this author at the Department of Building and Construction Techniques Engineering, Al-Mustaqbal University, 51001, Hilla, Iraq; E-mail: dr.riyadh.abdulabbas@uomus.edu.iq

Cite as: Alsultani R, Saber Q, Al-Saadi A, Mohammed O, Abed S, Naser R, Hussein A, Muslim F, Fadhil H, Karim I, Khassaf S. The Impact of Climate Change on the Reinforcement Durability of Concrete Bridge Structures. Open Civ Eng J, 2024; 18: e18741495337012. <http://dx.doi.org/10.2174/0118741495337012240812105905>



CrossMark

Received: July 03, 2024
Revised: July 27, 2024
Accepted: July 31, 2024
Published: October 09, 2024



Send Orders for Reprints to
reprints@benthamscience.net

1. INTRODUCTION

Human settlements require infrastructure to support

people's activities concerning buildings, transportation, electricity, water, and communications. For instance,

transportation infrastructure was centered around the Iraqi cities of Hilla and Baghdad and along the Middle Euphrates, which has a moderate temperature zone [1], as seen in Fig. (1), under the pattern of population distribution and industrial activity. Since concrete construction dominates the development of most key infrastructure, the nation's ability to provide basic services and economic activity depends heavily on its performance. Iraq is not unique in this regard; other countries with similar climates and reliance on physical infrastructure for their social and economic well-being are the US, Canada, and Europe. One of the primary elements that can drastically alter the long-term performance of concrete buildings is deterioration [2-4]. It is commonly recognized that the ongoing environmental conditions, in addition to the building techniques and material composition, have an impact on the pace of degradation of a structure during its service phase of life cycle. Climate change has the potential to affect this environment, particularly over the long run. It might speed up the degradation process and lead to corrosion cracking, which would need more costly and time-consuming repairs and weaken concrete buildings [5, 6]. Infrastructure development, maintenance, replacement, and renovation decisions need long-term planning and can have an impact for at least 30 to 200 years. Climate conditions in the future must be taken into account while making these choices and allocating funds. Therefore, understanding how climate change is affecting the country can help us protect human settlements and

national infrastructure as well as make decisions regarding possible future issues.

The Climate Change Assessment Report [4] states that there was a considerable rise in the atmospheric concentration of carbon dioxide from 280 ppm in 1750 to 380 ppm in 2005, with an increasing trend. As atmospheric CO₂ concentrations grow, the best estimate of the temperature increase since 1990 is 2.1°C per 550 ppm CO₂, 3.0°C per 700 ppm CO₂, and 4.4 °C per 1000 ppm CO₂ by 2100. This is contrasted with pre-industrial times [4]. Temperature will increase the rates of carbonation, corrosion, and chloride penetration.

Soudret *et al.* [6] developed spatial reliability models to predict the probability and extent of corrosion damage caused by carbonation; nevertheless, the analysis was based on a constant (constant over time) CO₂ concentration. The Fib code [7] chose a CO₂ concentration of about 500 ppm based on a linear rise of 1.5 ppm/year over 100 years. Nevertheless, corrosion onset was only taken into account in the limit scenario in this investigation.

According to Stewart *et al.*'s research [8], the ambient CO₂ concentration associated with a typical urban setting is between 5% and 10% greater than that of a rural one. The use of fossil fuels for transportation, residential heating, electricity production, and other reasons affects the concentration of CO₂ in metropolitan areas, where CO₂ concentrations are frequently greater and closer to ground

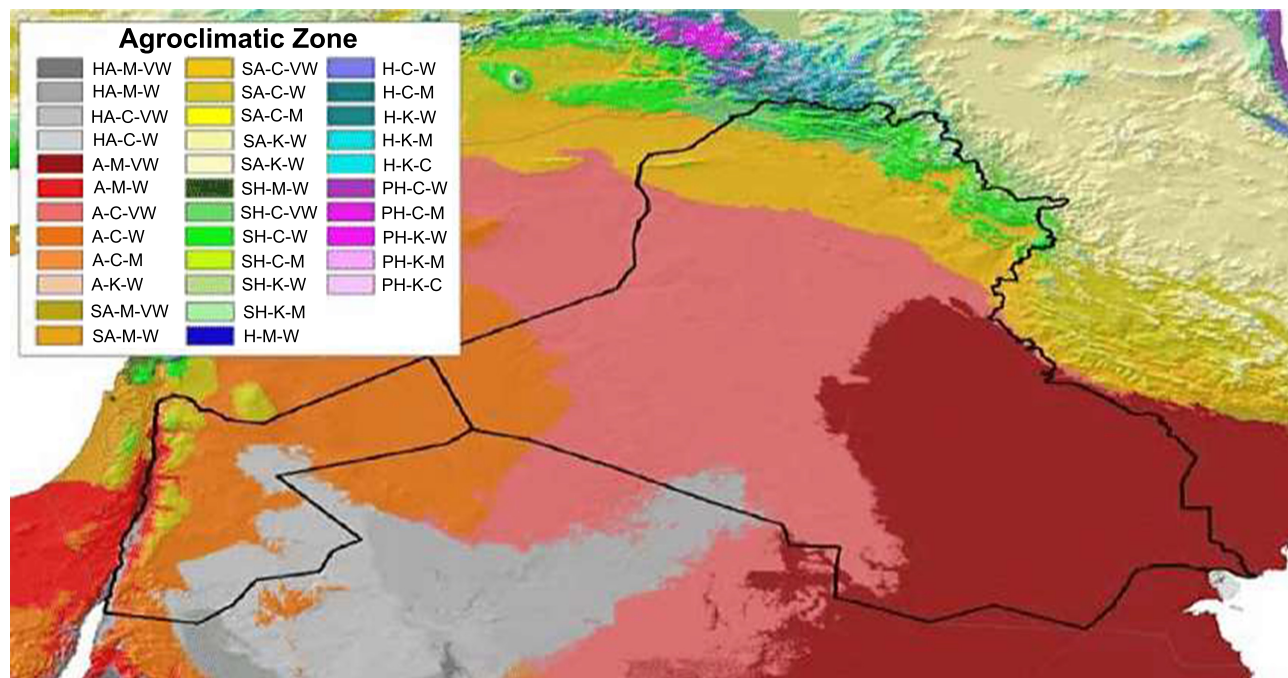


Fig. (1). Climatic of Iraqi zones [1].

level. Peng and Stewart [9] predicted the likelihood and severity of corrosion caused by carbonation, the degree of crack coverage, and integrity loss in prestressed and RC concrete beams under flexure and shear using the most recent CO₂ concentration data supplied by another study [4]. Then, in order to determine if increasing the design cover would be a financially sound modification to decrease the effects of concrete carbonation, Stewart and Peng [10] conducted a life cycle cost study. There also doesn't seem to have been any research done on how climate change impacts corrosion produced by chloride. Bastidas-Arteaga *et al.* [11] did, however, compute increases in the likelihood of corrosion onset owing to climatic change of 5% to 15%. Al-Hassan *et al.* [12] have emphasized the significant impact that climatic circumstances have on structural dependability.

Iraq's vulnerability to climate change and its impact on infrastructure is heightened compared to other regions due to several factors: significant temperature fluctuations with summer temperatures often exceeding 50°C accelerate concrete degradation through thermal expansion and contraction; severe water scarcity and high salinity levels in soil and water expedite the corrosion of steel reinforcement in concrete; political and economic instability restricts investment in infrastructure maintenance and upgrades, exacerbating susceptibility to deterioration; rapid urbanization in cities like Baghdad and Hilla increases strain on infrastructure and CO₂ emissions, intensifying the urban heat island effect; and outdated infrastructure, not designed for current and projected climate impacts, further increases vulnerability to accelerated deterioration and failure.

This paper introduces a reliable probabilistic methodology designed to predict three critical corrosion-related events in concrete infrastructure exposed to elevated CO₂ levels and increasing temperatures: (1) the probability of corrosion initiation, (2) the probability of corrosion-induced damage (such as severe cracking), and (3) the extent of corrosion-induced loss in steel reinforcement. Anticipated changes in atmospheric carbon dioxide concentration, temperature, and local humidity levels in Al-Hilla and Baghdad, representing temperate and tropical climates in Iraq respectively, are projected over the next century.

2. MATERIALS AND METHODS

This methodology combines scenario analysis, probabilistic techniques, and robust data validation to provide a comprehensive assessment of the impact of climate change on concrete infrastructure in Iraq. By understanding the potential future conditions and their implications, policymakers and engineers can develop more effective strategies for infrastructure resilience and adaptation.

2.1. Scenario Development

Four scenario groups A1, A2, B1, and B2 are developed to forecast the human effect of emissions concerning population, economics, technology, energy,

land use, and agriculture [13]. These scenarios are based on the Special Report on Emissions Scenarios (SRES) developed by the Intergovernmental Panel on Climate Change (IPCC).

2.1.1. Scenario A1

This scenario anticipates a peak in the world population mid-century, followed by a decline. It assumes rapid technological advancements and widespread adoption of efficient technologies. Regional differences in per capita income are expected to narrow significantly. It is relevant for understanding how advanced technology and global economic convergence can mitigate or exacerbate the impacts of climate change on infrastructure.

2.1.2. Scenario A2

This scenario envisions a highly diversified world where local identities are preserved. Population growth continues to rise, economic development is concentrated in certain regions, and per capita economic growth becomes more distributed. Technological innovation occurs but is unevenly distributed. A2 helps in assessing the impact of local economic and technological disparities on infrastructure vulnerability.

2.1.3. Scenario B1

It assumes the same population trend as A1 but emphasizes the development of clean, resource-efficient technologies and a shift from a material-intensive to an information- and service-based economy. It is critical to evaluate the potential benefits of sustainable technologies and economic practices on infrastructure resilience.

2.1.4. Scenario B2

It predicts slower global population growth than A2 and assumes more varied and slower intermediate stages of economic and technological development than B1 and A1. It places less emphasis on global approaches to sustainability than B1 and A1. This scenario explores the implications of moderate economic and technological progress combined with slower population growth on infrastructure.

2.2. Probabilistic Techniques

To predict the impact of elevated CO₂ levels and increasing temperatures on concrete infrastructure, a probabilistic methodology is employed. The primary probabilistic techniques include:

2.2.1. Monte Carlo Simulation

This technique is used to model the uncertainty and variability in the input parameters, such as CO₂ concentration, temperature, and relative humidity. By running thousands of simulations, a distribution of possible outcomes is obtained, providing insights into the likelihood of different levels of infrastructure degradation.

2.2.2. Reliability Analysis

The methodology incorporates reliability analysis to

estimate the probability of failure of concrete structures due to corrosion. This involves defining a limit state function that describes the boundary between safe and failed states of the structure [14, 15].

2.2.3. Time-Dependent Analysis

The models account for the time-dependent nature of environmental factors and material properties. For instance, relative humidity is expressed as a function of time:

$$RH(t) = RH(2000) + RH_{mid} \times T_{mid}(t) \quad (1)$$

where $T_{mid}(t)$ is the average global rising temperature concerning emission assumptions.

2.3. Assumptions and Model Parameters

2.3.1. CO₂ Concentration

Future CO₂ concentrations are modeled based on historical data and projected trends under each scenario. The urban CO₂ concentration is assumed to be higher than in rural areas, consistent with findings by George *et al.* [16].

2.3.2. Temperature and Humidity

The temperature increase is assumed to follow the projections provided by the IPCC for each scenario. Relative humidity is modeled as a function of temperature increase, with RH_{mid} representing the change in relative humidity per degree of global warming.

2.3.3. Qurban Factor

Given the lack of statistical information, a normal distribution with a mean of 1.15 and a coefficient of variation of 0.10 is used for the Qurban factor, which represents the increased degradation rate in urban environments.

2.4. Machine Learning Model

In this study, machine learning models, including Gaussian Process Regression and various regression techniques, were employed to predict corrosion levels in concrete structures under different emission scenarios and environmental conditions. These models were selected due to their capability to manage complex, non-linear relationships between the input variables and the corrosion outcomes.

The input parameters for the models included atmospheric CO₂ levels, which were derived from historical data and future projections. Temperature variations were based on General Circulation Models (GCMs) that provided temperature data and future projections. Relative humidity was considered with both historical records and projected changes. Additionally, exposure classifications were included, such as A1, A2, B1, and B2, representing different scenarios for carbonation and chloride exposure.

The output parameters of the models included the probability of corrosion initiation, which indicates the

likelihood of corrosion beginning under specified conditions. Corrosion-induced damage was assessed to measure the extent of damage resulting from corrosion. The models also estimated the corrosion loss in steel reinforcement, reflecting the reduction in the diameter of reinforcing bars due to corrosion.

The dataset used for training the models was generated through simulations of corrosion data, utilizing historical climate data and future projections from GCMs. This dataset incorporated various environmental variables and emission scenarios. To evaluate the model's performance, the dataset was split into training and validation subsets. Random sampling was employed to ensure that the training and validation sets represented a broad range of conditions, facilitating a comprehensive evaluation of the model's accuracy.

2.5. Data Sources and Validation

2.5.1. Climate Data

Temperature and CO₂ concentration data are sourced from the IPCC and other climate models. Historical data are validated against observed records to ensure accuracy.

2.5.2. Infrastructure Data

Data on concrete structures, including material properties and historical degradation rates, are collected from national and international engineering databases.

2.5.3. Urbanization Data

Information on urban growth and pollution levels is obtained from governmental and research institutions.

2.6. Limitations and Uncertainties

2.6.1. Data Accuracy

There may be discrepancies in historical data due to measurement errors or incomplete records. Efforts are made to cross-validate data from multiple sources to mitigate this issue.

2.6.2. Model Assumptions

The assumptions made regarding future trends in CO₂ concentration, temperature, and technological development introduce uncertainty into the projections. Sensitivity analyses are conducted to understand the impact of these assumptions on the results.

2.6.3. Local Variability

The models may not fully capture local variations in climate and environmental conditions. Regional studies are recommended to supplement the findings and provide more localized assessments.

Current research offers several technical improvements over current methods by incorporating a comprehensive set of input parameters, such as detailed atmospheric CO₂ levels, temperature variations from General Circulation Models (GCMs), relative humidity, and various exposure classifications. Unlike traditional models,

which often rely on limited variables and linear approaches, our study employs advanced machine learning techniques like Gaussian Process Regression to capture complex, non-linear relationships and provide more accurate predictions. This includes precise forecasts of corrosion initiation, damage, and loss in steel reinforcement. Additionally, our rigorous training and validation processes, including k-fold cross-validation, ensure robust model performance and higher accuracy compared to conventional methods, as evidenced by significantly improved coefficients of determination (R^2) and reduced Root Mean Square Error (RMSE) values.

3. CARBONATION INDUCED CORROSION

3.1. Time to Corrosion Initiation

Numerous variables, including concrete quality, concrete cover, relative humidity, ambient carbon dioxide concentration, and others, affect the depth of carbonation [17]. The effects of carbonation have been the subject of several investigations, and various mathematical models have been developed to predict the depths of carbonation (see, *e.g.*, [8, 18] for a review). It has been observed that corrosion may occur if there is less than a 1-2 mm gap between the carburizing contact and the reinforcing bar's surface [19]. However, probabilistic models that evaluate resilience design requirements frequently ignore this influence [7, 20]. Consequently, the corrosion initiation time (T_i) occurs when the concrete cover and the carbonation contact are equal. The carburizing depth model that DuraCrete [18] and Yoon *et al.* [19] supported takes into account a wide range of factors that affect the depth of carbonation. The diffusion coefficient will increase with temperature, raising the carburizing depths [20-23].

Data on the influence of time on the rate of corrosion of gaseous reinforced concrete buildings are few. Therefore, the current study for carburization assumes a constant rate of corrosion throughout time. This is probably a cautious assumption since, as rust products build up and impede the corrosion process, the corrosion rate will usually decrease with time [24].

3.2. Corrosion Propagation

A study of wear rates and models may be found in a study [25-29]. The rate at which carbonization produces corrosion varies and is primarily based on exposure and climatic conditions. There are several empirical models out there, but they only pay attention to certain aspects. It is important to note that insufficient oxygen or water might cause corrosion to eventually stop. Actually, high humidity in concrete can impede oxygen from entering the corrosion zone and slow down the reinforcement's corrosion process. Dry concrete with low water content can also prevent corrosion from occurring. Relative humidity $RH_{(t)}$ less than 50%, as in a study [30, 31], makes carbonates and chlorides less prone to corrosion. According to this study, $0.1 \mu\text{A}/\text{cm}^2$ of corrosion current density (i_{corr}) and a corrosion rate of $1 \mu\text{A}/\text{cm}^2 = 0.0116 \text{ mm}/\text{year}$ correspond to minimal corrosion. The optimal

relative humidity range for corrosion is 70% to 80% [31]. DuraCrete gave the statistical values at a temperature of 20°C , and it is believed that the wear rate in this study is normally distributed [18]. According to DuraCrete's model, the rate of corrosion will rise with temperature [24, 20].

Data on the influence of time on the rate of corrosion of gaseous reinforced concrete buildings are few. Therefore, the current study for carburization assumes a constant rate of corrosion throughout time. This is probably a cautious estimate since, as rust products build up and impede the corrosion process, the corrosion rate will typically decrease over time [32].

4. CHLORIDE INDUCED CORROSION

4.1. Chloride Penetration Model

Fick's second law of diffusion is used to measure the penetration of chlorides through experimentation. Nevertheless, the field circumstances and mechanisms of chloride penetration are not the same as those considered by Fick's law; for a discussion [33]. However, due to its computational ease, Fick's law is frequently employed to explain the penetration of chlorides into concrete. Specifically, by fitting Fick's law to the observed chloride cross sections, one can quickly compute the diffusion coefficients (D_c) and surface chloride concentration (C_s). To determine the chloride concentration, an enhanced model based on DuraCrete's time-dependent chloride diffusion coefficient [24] is employed.

According to available data, carbonation increases the concentration of free chloride in the pore solution by upsetting the balance between bound and free chlorides in the concrete. This, together with sulfur dioxide and nitrogen oxides, appears to hasten the action of chlorides. Nonetheless, it seems that no practical quantitative models have been developed based on these findings. As a result, the impact of the current study's interaction between carbonation and chlorides has been temporarily excluded.

The prevailing belief is that the concentration of surface chloride (C_s) remains constant over time, meaning that the amount of exposure to chlorides in a particular structural element won't alter from one year to the next. However, wet/dry cycles, rainfall patterns, wind patterns, and other factors may alter as a result of climate change. However, there is no evidence to back up how this impacts C_s . There are three distinct exposure categories into which surface chloride concentration may be categorized: submerged zone, spray and tidal zone, and atmospheric zone. The critical chloride concentration is terminated at $0.35 \text{ kg}/\text{m}^3$ and has a normal distribution with a mean and COV of $3.35 \text{ kg}/\text{m}^3$ and $0.375 \text{ kg}/\text{m}^3$, respectively [34]. The quality of the concrete has no bearing on the critical chloride concentration [24]. According to available data, carbonation increases the concentration of free chloride in the pore solution by upsetting the balance between bound and free chlorides in the concrete. This, together with sulfur dioxide and nitrogen oxides, appears to hasten the action of chlorides. However, it appears that these results

have not led to the development of any useful quantitative models. Thus, the effect of the interaction between chlorides and carbonation in the current investigation has been temporarily omitted.

4.2. Corrosion Propagation

The concrete's grade, cover, and environment all affect corrosion rates, which are quite varied. For instance, the British Standard BS 6349-1 [35] indicates that the mean corrosion rate is $3.45 \mu\text{A}/\text{cm}^2$ for the atmospheric zone, $6.9 \mu\text{A}/\text{cm}^2$ for the splash zone, and $3.45 \mu\text{A}/\text{cm}^2$ for the tidal zone at $0.04 \text{ mm}/\text{yr}$. The DuraCrete recommended corrosion rates [18]. This presumption is cautious. Diana Software models the impact of temperature on corrosion rate [35].

5. TIME TO CORROSION DAMAGE

Damage and cover cracking brought on by corrosion develop on the concrete surface above and parallel to the rebars. Three stages can be used to characterize the different phases of crack growth:

- (i) T_i is corrosion initiation;
- (ii) T_{1st} is time to first cracking; a hairline crack with a width of 0.05 mm ; and
- (iii) T_{sev} is time for the crack to propagate from crack initiation to a limited crack width.

The time to corrosion damage (severe cracking or spalling):

$$T_{sp} = T_i + T_{1st} + T_{sev} \quad (2)$$

The corrosion products must first fill the porous zone surrounding the steel reinforcing bar before they start to apply internal pressure to the nearby concrete. Thus, not every product of corrosion causes expanding stress in concrete. El-Maadawi and Soudaki [36] employed this strategy for crack initiation, and their model is applied here. Typically, the thickness of the porous zone (δ_o) falls between 10 and $20 \mu\text{m}$. It may be represented by a normal distribution with a mean of $15 \mu\text{m}$ and a coefficient of variation of 0.1 . It should be highlighted that the precision of the corrosion initiation time (T_i) determines the severity of cracking time. and the duration (T_{sev}) between the crack initiation and maximum crack width, meaning that service life estimates are largely unaffected by the crack initiation model [2]. The point at which the fissure in the concrete cover widens to a maximum of one millimeter is known as the severe cracking time. A model of the crack propagation rate that takes into account the time needed for crack growth from fracture initiation to maximum crack width (T_{sev}) was created by Mollard and Stewart [37]. The duration (post-initiation) required for the concrete surface to begin to fracture and attain a crack width of $w \text{ mm}$.

6. RESULTS AND DISCUSSION

Iraq's environmental exposure is divided into three climate zones: tropical, temperate, and arid. Particularly

when it comes to characterizing the anticipated temperature fluctuations, the two climates that the selected sites in Hilla and Baghdad depict are temperate and tropical, respectively, and are not very different from the exposed structures.

On the other hand, local factors associated with microclimate include the position of structural features about changeable water levels (and the period at which this happens) and the concentration of sulfates, pH, and chlorides in the water or soil. Concrete that is wet or has low relative humidity indoors is frequently less susceptible to carbonation. Concrete outdoors and inside with moderate to high air humidity are subject to long-term, sporadic contact with water. Concrete covered by rain is highly vulnerable to carbonation. Structures in marine areas are less prone to corrode than those exposed to spray and tides if they are continually submerged or exposed to salt air but are not in direct contact with seawater. Due to these factors, the reliability analyses that will be conducted will concentrate on corrosion predictions for structures that are exposed to chlorides and carbonation, respectively, and for those that are not. The minimum concrete cover and concrete compressive strength are related to the durability design standards outlined in AS3600, which also assume conventional formwork and compression.

Figs. (2 and 3) display the probability of corrosion start and damage for each emission scenario and exposure categorization. Impact of temperature predictions on the likelihood of corrosion damage and commencement for exposure category A1. The likelihood of corrosion initiation is less than 0.004 and the possibility of corrosion damage is less than 0.002 for exposure categories B2 and C. These odds are modest regardless of the emissions scenario. Exposure categories A1, A2, and B1 pose the greatest risk of corrosion initiation and damage because they are the most carbonation-prone exposures; exposure classes other than these are more directly associated with coastal chloride exposure. Within the first 20 to 30 years of service life, significant corrosion damage is unlikely to occur; however, for scenarios with emissions of 550 ppm or more, the likelihood of corrosion damage increases to 20% to 40% after that.

This means that practically speaking, 20% to 40% of all concrete surfaces should be expected to be damaged by 2100 and require maintenance or replacement. In the worst-case scenario, the chance of corrosion damage is up to 460% greater than in the reference (best) mitigation scenario. This suggests that over the service life of many concrete buildings, elevated CO_2 concentrations might result in a large possibility and amount of corrosion damage that may require expensive and damaging repairs.

Because carbonation causes very low corrosion rates and takes a considerable time to begin, the corrosion loss of reinforcement diameter is quite small. For instance, the average extra corrosion loss for Baghdad and Hilla under the emission scenario and exposure A2 at year 2100 (in comparison to the corrosion loss for the reference

mitigation scenario) is 0.23 and 0.08 mm, respectively. They have the highest corrosion loss for any exposure. For a bar with a diameter of 16 mm, this means a 2.8% and 1.0% reduction in cross-sectional area, respectively, and a corresponding loss in structural capabilities. For emission scenarios, different exposure classes, and reinforcing bars with a larger diameter, the proportional drop in the cross-sectional area reduces even more.

As indicators of performance for the corrosion model, the coefficient of correlation and RMSE were chosen. Typically, the coefficient of determination refers to the percentage of the response variable's variance that the used model can account for RMSE values between 0.2 and

0.5, as a general rule, indicating that the model can predict the data quite correctly. A modified R-square of greater than 0.75 is also a very good value for demonstrating accuracy. It took 556.20 seconds to learn. The hardware specs were an NVIDIA GeForce GTX 960 and an Intel i7-7700K CPU running at 4.20GHz.

The training and RMSE data's coefficients of determination were 0.6377 and 0.4722, respectively. In contrast, the validation data's coefficient of determination was 0.5035 and its RMSE was 0.4683. The coefficients of prediction therefore exceeded 0.75 for both the one used for training and validation datasets. The training as well as validation results are shown in Table 1 and Fig. (4).

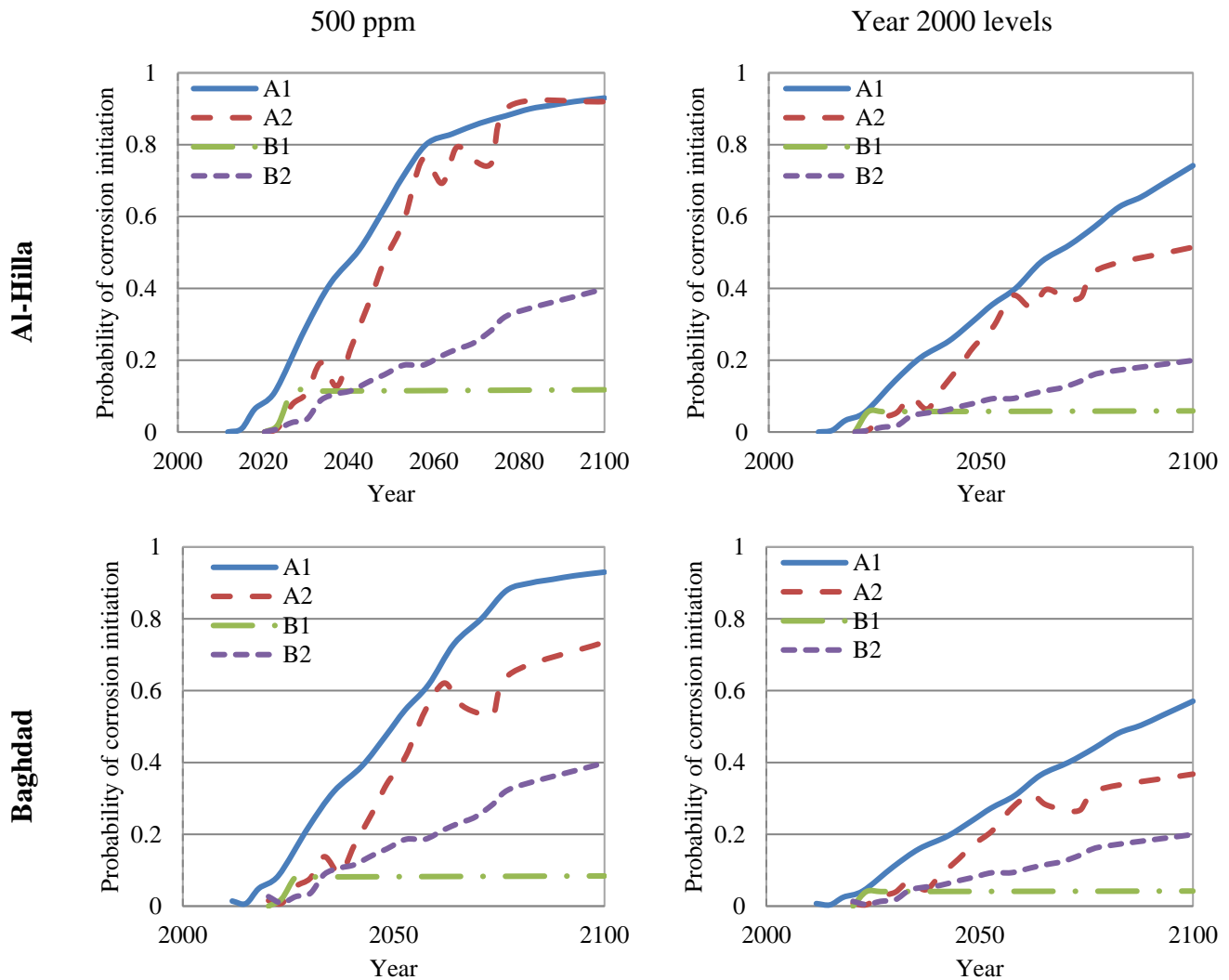


Fig. (2). Probabilities of carbonation-induced corrosion initiation for Hilla and Baghdad.

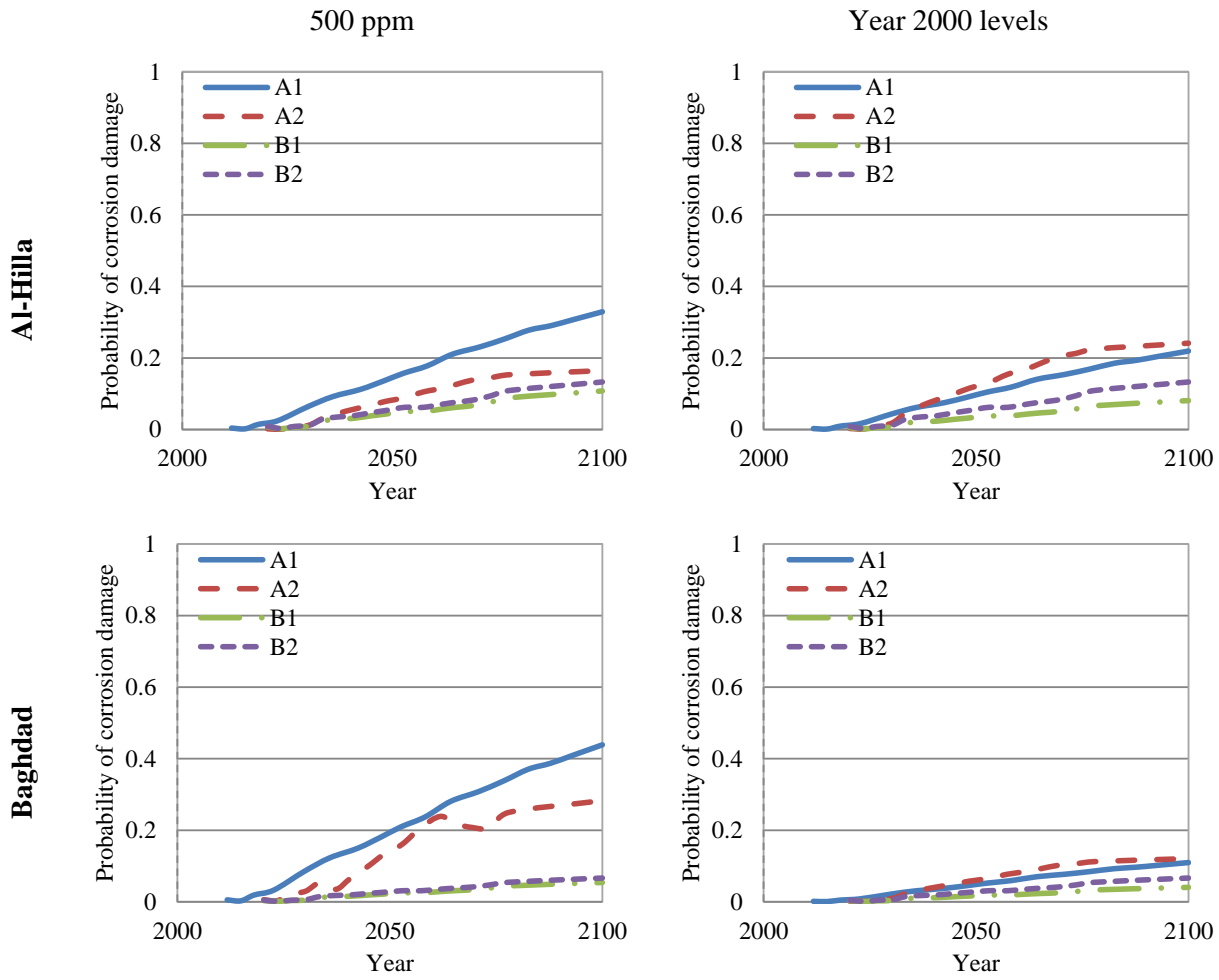


Fig. (3). Probabilities of carbonation-induced corrosion damage, for Hilla and Baghdad.

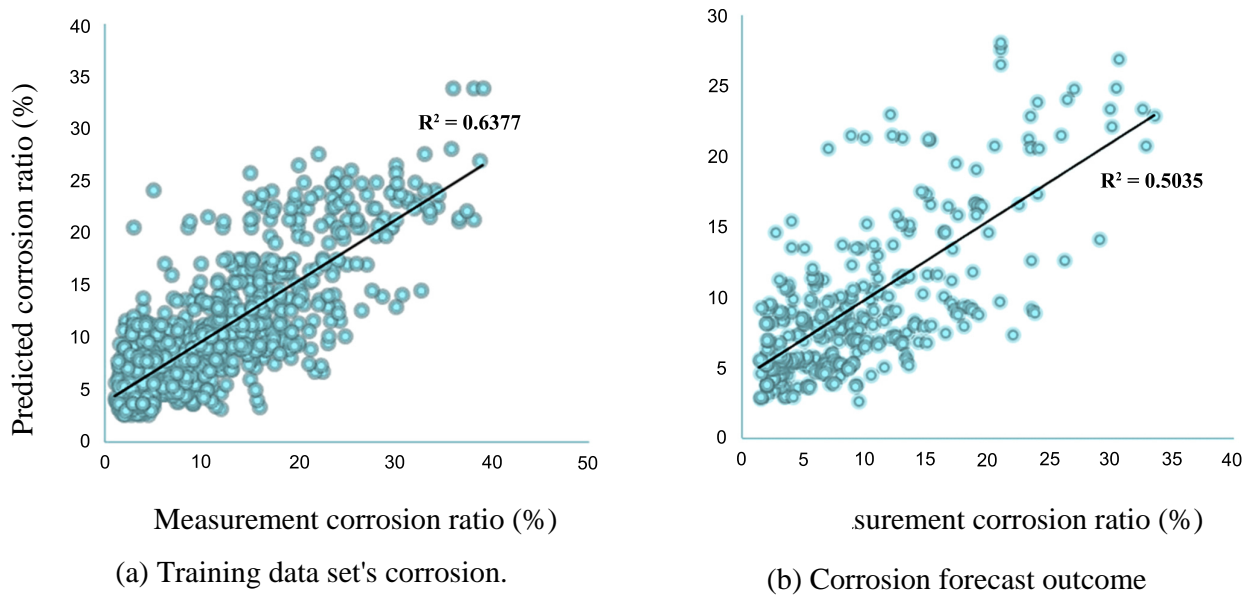


Fig. (4a, b). Corrosion estimation outcome of the proposed model.

Table 1. Performance indicators for corrosion models.

| Performance Indicator | Value |
|--------------------------|--------|
| Training dataset R^2 | 0.6377 |
| Training dataset RMSE | 0.4722 |
| Validation dataset R^2 | 0.5035 |
| Validation dataset RMSE | 0.4683 |

| | Dataset #1 | Dataset #1 | Dataset #1 | Dataset #1 | Dataset #1 | Results (R^2) |
|----------|------------|------------|------------|------------|------------|-------------------|
| Split #1 | Validation | Training | Training | Training | Training | 0.904 |
| Split #2 | Training | Validation | Training | Training | Training | 0.956 |
| Split #3 | Training | Training | Validation | Training | Training | 0.848 |
| Split #4 | Training | Training | Training | Validation | Training | 0.916 |
| Split #5 | Training | Training | Training | Training | Validation | 0.890 |

Fig. (5). Results of the suggested model's k-fold validation test.

Table 1 presents the R^2 values, indicating model performance. The R^2 value of 0.5 for the validation dataset suggests moderate predictive accuracy. It can be acknowledged that a higher R^2 value (around 0.8) is generally preferred for indicating good model performance. To improve this, we are optimizing the model by refining input features and exploring advanced machine-learning techniques.

Cross-validation was done to make sure the suggested model fit. When a data set is tiny in size, cross-checking determines whether the data set is overfitted. The validation process employed the k-fold approach. The training dataset was divided into four folds using the k-fold cross-validation, and the validation dataset had five folds in total. The distribution strategy was selected at random. The results of the entire study are shown in Fig. (5). There was minimal difference between the first experimental result (0.5028) and the average validation result. This result demonstrated that the experimental results were inappropriate for a certain set of data. This inconsistency highlights that the model performed poorly for these particular data sets, indicating potential limitations in the model's accuracy or its generalizability to all data conditions. Further investigation is necessary to understand the causes of these discrepancies and to refine the model for improved performance across diverse datasets.

The majority of investigations are based on the diffusion theory, which is based on Fick's second rule, which indicates that concrete corrosion is inversely related to time

squared [28-30]:

$$C_t = k\sqrt{t} \quad (3)$$

Where C_t denotes the carbonation depth, k indicates the coefficient of carbonation rate, and t represents the exposure time. Here, k is the most important coefficient that determines the corrosion rate [38].

The suggested approach was contrasted with the current equation-based corrosion model, where the mathematical equation was created using the same data set as the corrosion coefficient as stated in Eq. (3).

Even if previous research has computed coefficients, the coefficient that was generated in this study has been tailored for the data to reach the greatest feasible index of performance. Erosion equations and indicators were developed independently for each location due to the differences in environmental variables within each.

The proposed model was compared with existing equation-based corrosion models and the test findings are summarized in Table 2. The coefficients of determination for the proposed model were significantly higher (0.876 for Al-Hilla and 0.885 for Baghdad) than those for the equation-based model (0.426 and 0.542, respectively). Other regression analysis techniques, such as linear regression, regression trees, support vector machines, and Gaussian process regression, were also evaluated. The proposed model outperformed these methods, with the highest determination coefficient (0.4310) among the alternatives.

Table 2. Simulating corrosion using the proposed model.

| Region | Methodology | R ² | RMSE |
|----------|----------------------------|----------------|-------|
| Al-Hilla | Proposed model | 0.876 | 0.497 |
| | Fick's second law equation | 0.426 | 4.95 |
| Baghdad | Proposed model | 0.885 | 0.485 |
| | Fick's second law equation | 0.542 | 5.556 |

Table 3. Results of alternative techniques' predictions using the corrosion model.

| Regression Analysis Method | | Validation Dataset | |
|-----------------------------|---------------------|--------------------|-------|
| | | R ² | RMSE |
| Linear regression | Normal | 0.135 | 7.478 |
| | Interaction | 0.225 | 7.105 |
| | Robust | 0.133 | 7.594 |
| | Stepwise | 0.214 | 7.136 |
| Tree | Complex | 0.395 | 6.342 |
| | Medium | 0.343 | 6.554 |
| | Simple | 0.220 | 7.140 |
| Support vector machine | Linear | 0.128 | 7.763 |
| | Quadratic | 0.251 | 7.074 |
| | Cubic | 0.227 | 7.397 |
| | Fine Gaussian | 0.383 | 6.407 |
| Gaussian process regression | Squared exponential | 0.430 | 6.143 |
| | Matern 5/2 | 0.432 | 6.134 |
| | Rational quadratic | 0.440 | 6.087 |

Other regression analysis techniques, such as linear regression, regression trees, support vector machines, and Gaussian process regression, were contrasted with the suggested approach.

The identical training and validation datasets were used by all regression analysis techniques. The performance findings of the various regression analysis techniques are summarized in Table 3. The Boolean quadratic approach with the Gaussian regression process had the greatest determination coefficient (0.4310) among the regression analysis methods. The determination coefficient for the proposed erosion model was 16.8% more than that for the Gaussian process regression.

The findings of this study corroborate earlier research on the impacts of increased CO₂ levels on concrete structures. For instance, Stewart *et al.* (2018) observed that elevated CO₂ concentrations in urban areas lead to higher carbonation rates in concrete, consistent with our results that demonstrate increased corrosion risk in urban settings. Similarly, George *et al.* (2020) highlighted urban-rural disparities in CO₂ concentrations, which aligns with our findings that urban areas face significantly higher carbonation risks.

However, this study extends beyond these previous works by incorporating a probabilistic approach to model corrosion under varying emission scenarios, providing a more nuanced understanding of the long-term impacts of climate change on concrete infrastructure. Unlike earlier studies that often used deterministic models or genera-

lized predictions, our probabilistic models account for uncertainties and variability in environmental conditions, offering a more comprehensive risk assessment. Additionally, this study includes a detailed analysis of specific exposure classifications (A1, A2, B1, B2) and their relevance to the Iraqi context, highlighting the particular vulnerability of regions like Hilla and Baghdad to corrosion and structural damage.

In contrast to the broader trends identified by previous research, our study provides specific predictions on the likelihood and extent of corrosion damage in concrete structures based on localized climatic data and emission scenarios. This detailed approach allows for more targeted recommendations for infrastructure management and maintenance, addressing gaps in earlier studies that may have lacked region-specific insights.

In the end, the current proposed framework enhances predictive accuracy for concrete corrosion by integrating advanced machine learning techniques with comprehensive data, including atmospheric CO₂ levels, temperature projections from General Circulation Models (GCMs), relative humidity, and various exposure classifications. This approach surpasses traditional models by capturing complex, non-linear relationships and providing more precise forecasts of corrosion initiation, damage, and loss. Implementing this framework in real-world applications is possible by collecting detailed environmental data, training machine learning models using rigorous validation techniques, and applying these models to

predict and manage infrastructure integrity. This strategy ensures robust, reliable predictions and supports informed decision-making for infrastructure maintenance and planning.

7. PRACTICAL APPLICATIONS AND FURTHER RESEARCH

For concrete infrastructure with exposure ratings of B1, B2, and C that is situated within 50 kilometers of Al-Hilla and Baghdad, corrosion from carbonation is extremely low to nonexistent. However, in inland dry or temperate climatic regions (A1 and A2), the probability of corrosion damage can reach 20%-40% (Fig. 2), and the risk of damage can grow by 40%-460% due to climate change (Fig. 3). Fortunately, only a small percentage of Iraq's infrastructure is located in these areas; yet, infrastructure of this kind may require appropriate and reasonably priced adaptation techniques. There is a very significant danger of damage from chloride corrosion due to the heavy spray and exposure of maritime structures in tidal water.

The fact that there is a significant chance of corrosion damage even under the reference mitigation scenario—which assumes that CO₂ levels in 2000 would remain constant throughout time is pertinent to our debate. The findings are predicated on the durability design parameters, which solely address the concrete's compressive strength and minimum concrete cover. It is crucial to remember that precise findings about the influence of climate change and the likelihood of damage to a certain structure can only be reached by taking into account the structural features, orientation, structural classification, and other information unique to that structure. An economic assessment of adaption measures, such as improved cover, more durable concrete mix or stainless steel reinforcement, and coatings, is necessary to maintain concrete infrastructure in an efficient manner for the next 100 years. A preliminary economic review has been carried out to broaden the design scope, but much more research remains.

CONCLUSION

This study employed time-dependent reliability analysis to assess the probabilities of corrosion initiation and corrosion-induced damage in current concrete infrastructure under changing climatic conditions up to the year 2100. Additionally, the extent of reinforcement cross-sectional loss was calculated. Projections for the next century indicate expected changes in local temperature, humidity, and atmospheric carbon dioxide concentration in Al-Hilla and Baghdad, representing temperate and tropical regions in Iraq, respectively. Scenarios considered temperature and humidity levels remaining below 550 ppm, consistent with year 2000 levels, along with various carbon dioxide emission scenarios, including a best-case" scenario where CO₂ levels remain steady at 2000 levels. The probabilistic study accounted for uncertainties related to CO₂ content, material properties, dimensions, degradation processes, and forecast models.

Key findings include:

1. In dry or moderate inland climates in Iraq, the risk of damage from carbonation may increase by over 400% by 2100.
2. The maximum increase in the risk of damage from chloride corrosion is 15%, with reinforcement corrosion loss limited to 9.5%.
3. Results indicate higher susceptibility to rises in atmospheric CO₂ levels.
4. Coefficients for the recommended carbonation model were determined as 0.426 and 0.542 for Al-Hilla and Baghdad, respectively.
5. The coefficients of determination for the equation-based erosion model were found to be 0.129 and 0.035 for the selected locations.
6. The suggested model outperformed the corrosion index based on a formula.

Structures located in temperate or inland desert regions of Iraq are identified as the most susceptible. Therefore, appropriate and cost-effective adaptation measures may be necessary for these structures to ensure their durability in the face of changing climatic conditions.

AUTHORS' CONTRIBUTION

Riyadh Alsultani, Qahtan Adnan Saber, and Saleh I. Khassaf were involved in study conception and design, Qahtan Adnan Saber, Ahmed Ashor Al-Saadi and Omran I Mohammed collected the data, analysis and interpretation of results were performed by Riyadh Alsultani, Raghda Ali Naser, Alaa Hussein, Haneen Fadhil and Ibtisam R. Karim, manuscript was drafted by Riyadh Alsultani. All authors reviewed the results and approved the final version of the manuscript.

LIST OF ABBREVIATIONS

- IPCC = Intergovernmental Panel on Climate Change
 GCMs = General Circulation Models
 RMSE = Root Mean Square Error
 RH_(t) = Relative humidity
 (D_c) = Diffusion coefficients
 C_o = chloride concentration

CONSENT FOR PUBLICATION

Not applicable.

AVAILABILITY OF DATA AND MATERIALS

The data and supportive information are available within the article.

FUNDING

None.

CONFLICT OF INTEREST

The authors declare no conflict of interest financial or otherwise.

ACKNOWLEDGEMENTS

The corresponding author extends his thanks to Al-Mustaqbal University for the financial support for the research.

REFERENCES

- [1] P. Croce, P. Formichi, and F. Landi, "Influence of reinforcing steel corrosion on life cycle reliability assessment of existing RC buildings", *Buildings*, vol. 10, no. 6, p. 99, 2020. [<http://dx.doi.org/10.3390/buildings10060099>]
- [2] Y Mao, Y Zhu, CM Deng, S Sun, and DH Xia, "Analysis of localized corrosion mechanism of 2024 aluminum alloy at a simulated marine splash zone", *Eng. Fail. Anal.*, vol. 142, p. 106759, 2022. [<http://dx.doi.org/10.1016/j.engfailanal.2022.106759>]
- [3] D. Luo, F. Li, and G. Xing, "Corrosion resistance of 6061-T6 aluminium alloy and its feasibility of near-surface reinforcements in concrete structure", *Rev. Adv. Mater. Sci.*, vol. 61, no. 1, pp. 638-653, 2022. [<http://dx.doi.org/10.1515/rams-2022-0048>]
- [4] *Fourth assessment report of the intergovernmental panel in climate change*, Cambridge University Press: UK, 2007.
- [5] S. Zaghian, B. Martín-Pérez, and H. Almansour, "FEM of bridge piers subjected to eccentric load combined with reinforcement corrosion", *Eng. Struct.*, vol. 283, p. 115822, 2023. [<http://dx.doi.org/10.1016/j.engstruct.2023.115822>]
- [6] B. Sudret, G. Defaux, and M. Pendola, "Stochastic evaluation of the damage length in RC beams submitted to corrosion of reinforcing steel", *Civ. Eng. Environ. Syst.*, vol. 24, no. 2, pp. 165-178, 2007. [<http://dx.doi.org/10.1080/10286600601159305>]
- [7] "Model Code for Service Life Design", Available from: <https://www.fib-international.org/publications/fib-bulletins/model-code-for-service-life-design-pdf-detail.html>
- [8] M.G. Stewart, X. Wang, and M.N. Nguyen, "Climate change impact and risks of concrete infrastructure deterioration", *Eng. Struct.*, vol. 33, no. 4, pp. 1326-1337, 2011. [<http://dx.doi.org/10.1016/j.engstruct.2011.01.010>]
- [9] J. Peng, and M.G. Stewart, *Carbonation-induced corrosion damage and structural safety for concrete under enhanced greenhouse conditions. Research report no. 270.11.2008.*, The University of Newcastle: NSW, Australia, 2008.
- [10] M.G. Stewart, and J. Peng, "Life cycle cost assessment of climate change adaptation measures to minimise carbonation-induced corrosion risks", *Int J Eng Under Uncertain Hazards Assess Mitigation*, vol. 2, no. 1-2, pp. 35-46, 2010.
- [11] E. Bastidas-Arteaga, A. Chateauneuf, M. Sánchez-Silva, P. Bressolette, and F. Schoefs, "Influence of weather and global warming in chloride ingress into concrete: A stochastic approach", *Struct. Saf.*, vol. 32, no. 4, pp. 238-249, 2010. [<http://dx.doi.org/10.1016/j.strusafe.2010.03.002>]
- [12] J. El Hassan, P. Bressolette, A. Chateauneuf, and K. El Tawil, "Reliability-based assessment of the effect of climatic conditions on the corrosion of RC structures subject to chloride ingress", *Eng. Struct.*, vol. 32, no. 10, pp. 3279-3287, 2010. [<http://dx.doi.org/10.1016/j.engstruct.2010.07.001>]
- [13] *Emission scenarios. Special report of the intergovernmental panel on climate change.*, Cambridge University Press: UK, 2000. N. Nakicenovic, R. Swart, Eds.,
- [14] T.J.M. Alfatlawi, and R.A.A. Alsultani, "Characterization of chloride penetration in hydraulic concrete structures exposed to different heads of seawater: Using hydraulic pressure tank", *Engineering Science and Technology, an International Journal*, vol. 22, no. 3, pp. 939-946, 2019.
- [15] Z. Salahaldain, S. Naimi, and R. Alsultani, "Estimation and analysis of building costs using artificial intelligence support vector machine", *Mathematical Modelling of Engineering Problems*, vol. 10, no. 2, pp. 405-411, 2023. [<http://dx.doi.org/10.18280/mmep.100203>]
- [16] R. Alsultani, I.R. Karim, and S.I. Khassaf, "Dynamic response analysis of coastal piled bridge pier subjected to current, wave and earthquake actions with different structure orientations", *Int. J. Concr. Struct. Mater.*, vol. 17, no. 1, p. 9, 2023. [<http://dx.doi.org/10.1186/s40069-022-00561-5>]
- [17] R. Alsultani, I.R. Karim, and S.I. Khassaf, "Mathematical formulation using experimental study of hydrodynamic forces acting on substructures of coastal pile foundation bridges during earthquakes: As a model of human bridge protective", *Res Militaris*, vol. 12, no. 2, pp. 6802-6821, 2022.
- [18] "Modelling of Degradation: Duracrete, Probabilistic Performance Based Durability Design of Concrete Structures",
- [19] I.S. Yoon, O. Çopuroğlu, and K.B. Park, "Effect of global climatic change on carbonation progress of concrete", *Atmos. Environ.*, vol. 41, no. 34, pp. 7274-7285, 2007. [<http://dx.doi.org/10.1016/j.atmosenv.2007.05.028>]
- [20] R. Alsultani, and S.I. Khassaf, "Nonlinear dynamic response analysis of coastal pile foundation bridge pier subjected to current, wave and earthquake actions: As a model of civilian live", *Res Militaris*, vol. 12, no. 2, pp. 6133-6148, 2022.
- [21] J.M. Thair, A.D. Imad, and A.A. Riyadh, "Experimental determination and numerical validation of the chloride penetration in cracked hydraulic concrete structures exposed to severe marine environment", *IOP Conf. Series Mater. Sci. Eng.*, vol. 454, no. 1, p. 012099, 2018.
- [22] T.J.M. Alfatlawi, and R.A.A. Alsultani, "Determination of the Degree of Saturation and Chloride Penetration in Cracked Hydraulic Concrete Structures: Using Developed Electrical Conductivity Technique", *Indian J. Sci. Technol.*, vol. 11, p. 37, 2018.
- [23] M.A. Baccay, N. Otsuki, T. Nishida, and S. Maruyama, "Influence of cement type and temperature on the rate of corrosion of steel in concrete exposed to carbonation", *Corrosion*, vol. 62, no. 9, pp. 811-821, 2006. [<http://dx.doi.org/10.5006/1.3278306>]
- [24] T.J.M. Alfatlawi, N.J.A.L. Mansori, and R.A.A. Alsultani, "Stability assessment of diaphragm cellular cofferdams subjected to severe hydro-structural conditions", *Open Civ. Eng. J.*, vol. 14, no. 1, pp. 44-55, 2020. [<http://dx.doi.org/10.2174/1874149502014010044>]
- [25] H. Kada-Benameur, E. Wirquin, and B. Duthoit, "Determination of apparent activation energy of concrete by isothermal calorimetry", *Cement Concr. Res.*, vol. 30, no. 2, pp. 301-305, 2000. [[http://dx.doi.org/10.1016/S0008-8846\(99\)00250-1](http://dx.doi.org/10.1016/S0008-8846(99)00250-1)]
- [26] D. Russell, P.A.M. Basheer, G.I.B. Rankin, and E.A. Long, "Effect of relative humidity and air permeability on prediction of the rate of carbonation of concrete", *Proc.- Inst. Civ. Eng.*, vol. 146, no. 3, pp. 319-326, 2001.
- [27] H. Al-Khaiaf, and N. Fattuhi, "Carbonation of concrete exposed to hot and arid climate", *J. Mater. Civ. Eng.*, vol. 14, no. 2, pp. 97-107, 2002. [[http://dx.doi.org/10.1061/\(ASCE\)0899-1561\(2002\)14:2\(97\)](http://dx.doi.org/10.1061/(ASCE)0899-1561(2002)14:2(97))]
- [28] B. Bary, and A. Sellier, "Coupled moisture-carbon dioxide-calcium transfer model for carbonation of concrete", *Cement Concr. Res.*, vol. 34, no. 10, pp. 1859-1872, 2004. [<http://dx.doi.org/10.1016/j.cemconres.2004.01.025>]
- [29] M. Raupach, "Models for the propagation phase of reinforcement corrosion - an overview", *Mater. Corros.*, vol. 57, no. 8, pp. 605-613, 2006. [<http://dx.doi.org/10.1002/maco.200603991>]
- [30] J.N. Enevoldsen, C.M. Hansson, and B.B. Hope, "The influence of internal relative humidity on the rate of corrosion of steel embedded in concrete and mortar", *Cement Concr. Res.*, vol. 24, no. 7, pp. 1373-1382, 1994. [[http://dx.doi.org/10.1016/0008-8846\(94\)90122-8](http://dx.doi.org/10.1016/0008-8846(94)90122-8)]
- [31] A. Neville, "Chloride attack of reinforced concrete: An overview", *Mater. Struct.*, vol. 28, no. 2, pp. 63-70, 1995. [<http://dx.doi.org/10.1007/BF02473172>]

- [32] K.A.T. Vu, and M.G. Stewart, "Structural reliability of concrete bridges including improved chloride-induced corrosion models", *Struct. Saf.*, vol. 22, no. 4, pp. 313-333, 2000. [[http://dx.doi.org/10.1016/S0167-4730\(00\)00018-7](http://dx.doi.org/10.1016/S0167-4730(00)00018-7)]
- [33] D.V. Val, and M.G. Stewart, "Reliability assessment of ageing reinforced concrete structures-current situation and future challenges", *Struct. Eng. Int.*, vol. 19, no. 2, pp. 211-219, 2009. [<http://dx.doi.org/10.2749/101686609788220114>]
- [34] D.V. Val, and M.G. Stewart, "Life-cycle cost analysis of reinforced concrete structures in marine environments", *Struct. Saf.*, vol. 25, no. 4, pp. 343-362, 2003. [[http://dx.doi.org/10.1016/S0167-4730\(03\)00014-6](http://dx.doi.org/10.1016/S0167-4730(03)00014-6)]
- [35] "BS 6349-1:2000. Maritime Part 1: code of practice for general criteria, British Standard",
- [36] T. El Maaddawy, and K. Soudki, "A model for prediction of time from corrosion initiation to corrosion cracking", *Cement Concr. Compos.*, vol. 29, no. 3, pp. 168-175, 2007. [<http://dx.doi.org/10.1016/j.cemconcomp.2006.11.004>]
- [37] R.A.A.A. Al-Sultani, Z. Salahaldain, and S. Naimi, "Features of Monthly Precipitation Data Over Iraq Obtained by TRMM Satellite for Sustainability Purposes", <http://ajses.uomus.edu>
- [38] R. Alsultani, I. Karim, and S. Khassaf, "Dynamic response of deepwater pile foundation bridge piers under current-wave and earthquake excitation", *Engineering and Technology Journal*, vol. 40, no. 11, pp. 1589-1604, 2022. [<http://dx.doi.org/10.30684/etj.2022.135776.1285>]